Carbohydrate Polymers 225 (2019) 115203

Contents lists available at ScienceDirect

Carbohydrate Polymers

journal homepage: www.elsevier.com/locate/carbpol

Structure elucidation of a bioactive fucomannogalactan from the edible mushroom *Hypsizygus marmoreus*

Ruberney S. Oliveira[a,1], Stellee M.P. Biscaia[b,1], Daniel L. Bellan[b], Sthefany R.F. Viana[c], Maria Carolina Di-Medeiros Leal[d], Ana Flora D. Vasconcelos[e], Luciano M. Lião[d], Edvaldo S. Trindade[b], Elaine R. Carbonero[a,*]

[a] Departamento de Química, Universidade Federal de Goiás, Regional Catalão, 75704-020 Catalão, Brazil
[b] Departamento de Biologia Celular, Universidade Federal do Paraná, 81531-980 Curitiba, Brazil
[c] Departamento de Engenharia Rural, Faculdade de Ciências Agronômicas, Universidade Estadual Paulista "Júlio de Mesquita Filho", 18610-307 Botucatu, Brazil
[d] Laboratório de Ressonância Magnética Nuclear, Instituto de Química, Universidade Federal de Goiás, Campus Samambaia, 74001-970 Goiânia, Brazil
[e] Departamento de Química e Bioquímica, Faculdade de Ciências e Tecnologia, Universidade Estadual Paulista "Júlio de Mesquita Filho", 19060-900 Presidente Prudente, Brazil

ARTICLE INFO

Keywords:
Hypsizygus marmoreus
Mushroom
Fucomannogalactan
Chemical structure
Antimelanoma
B16-F10 cell

ABSTRACT

A fucomannogalactan (FMG-*Hm*), with a molecular weight of 17.1 kDa, obtained from fruiting bodies of *Hypsizygus marmoreus* exhibited promising *in vitro* antimelanoma effects. FMG-*Hm* was not cytotoxic, nor did it alter the cell morphology and proliferation, but was able to inhibit colony-forming ability and cell migration in B16-F10 murine melanoma cells. An analysis of the monosaccharide composition indicated that FMG-*Hm* was composed of fucose, mannose, and galactose in a ratio of 1.00:1.08:3.17. The FMG-*Hm* was structurally characterized based on methylation analysis, partial acid hydrolysis, and NMR experiments. The results indicated that FMG-*Hm* contained a α-(1→6)-linked galactopyranosyl main chain, partially substituted at O-2 by non-reducing ends of α-L-fucopyranose and β-D-mannopyranose. The predicted structure of the heteropolysaccharide was established as:

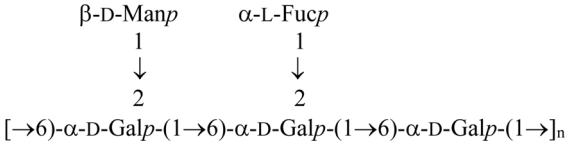

1. Introduction

Extracellular matrix (ECM) is a collection of macromolecules, forming a highly dynamic supramolecular network that undergoes continuous remodeling mediated by several matrix-degrading enzymes during normal and pathological conditions. The ECM components are interconnected to each other, and can also make connections with cell receptors forming a large network between cells and tissues (Theocharis, Skandalis, Gialeli, & Karamanos, 2016)

Deregulation of cell adhesion to the ECM is implicated at every step of tumorigenesis from initial hyperproliferation to local invasion, metastatic dissemination, and colonization to distant organs (Hamidi, Pietilä, & Ivaska, 2016). This ECM deregulation generates pores in the blood vessels and cell invasion with consequent metastasis to distant sites. In these new sites, they express ECM remodeling enzymes and create their new metastatic niches (Lu, Weaver, & Werb, 2012).

* Corresponding author.
E-mail addresses: ruberney_fds@hotmail.com (R.S. Oliveira), stellee.biscaia@gmail.com (S.M.P. Biscaia), daniellimabellan@yahoo.com.br (D.L. Bellan), sthefany.viana@yahoo.com.br (S.R.F. Viana), caroldimedeiros@gmail.com (M.C. Di-Medeiros Leal), ana.flora@unesp.br (A.F.D. Vasconcelos), lucianoliao@ufg.br (L.M. Lião), edstrindad@gmail.com (E.S. Trindade), elainecarbonero@gmail.com, elaine_carbonero@ufg.br (E.R. Carbonero).
[1] Both authors contributed equally to this work.

https://doi.org/10.1016/j.carbpol.2019.115203
Received 28 March 2019; Received in revised form 13 August 2019; Accepted 14 August 2019
Available online 17 August 2019
0144-8617/ © 2019 Elsevier Ltd. All rights reserved.

Thus, some markers of malignancy are used to evaluate the invasive capacity of tumor cells, since they are common features in the development of cancer, such as sustaining proliferative signaling, evading growth suppressors, resisting cell death, enabling replicative immortality, inducing angiogenesis, and activating invasion and metastasis. In this context, migration capacity is one of the most important markers as the first step towards metastasis (Hanahan & Weinberg, 2000, 2011).

Its highly invasive and metastatic capacity and subsequent rapid progression to death are characteristic of melanoma, which is among the 20 most commonly occurring cancer worldwide in men and women (WCRF International, 2019). The therapies currently available for this type of cancer are only palliative, increasing the survival of the patients but presenting numerous side effects (Maverakis et al., 2015). This fact, allied to the rising incidence and mortality of cancer, reinforces the need for research into new antitumor compounds.

In this context, several polysaccharides have been reported to have antitumor properties by cytotoxicity (Ivanova, Krupodorova, Barshteyn, Artamonova, & Shlyakhovenko, 2014; Ma et al., 2014; Ren, Wang, Guo, Yuan, & Yang, 2016; Srinivasahan & Durairaj, 2015); on the other hand, other authors demonstrated that the antitumor effects were do the alteration of markers of malignancy without toxicity (Biscaia et al., 2017; Milhorini et al., 2018; Tong et al., 2009).

Considering the diversity and specificity of the polysaccharides from macrofungi, as well as their importance as biological response modifiers (Meng, Liang, & Luo, 2016; Ren, Perera, & Hemar, 2012; Zong, Cao, & Wang, 2012), the medicinal mushroom *Hypsizygus marmoreus* ("white" strain) represents an important species to be studied, since the chemical structure and biological effects of its polysaccharides remain unexplored.

Our hypothesis in this work is that after isolating a new molecule from the mushroom *Hypsizygus marmoreus*, it presents antimelanoma activity, without causing toxicity, and thus, in the future, could avoid new side effects in adjuvant chemotherapeutic treatments.

For these purposes, in this study, a branched heteropolysaccharide was isolated and characterized and its biological effects were evaluated *in vitro* to determine its antimelanoma properties, using B16-F10 murine melanoma cells.

2. Material and methods

2.1. Extraction and purification of polysaccharides

The procedure for extraction and purification of polysaccharides from the *H. marmoreus* was similar to that described by Oliveira et al. (2018). Freeze-dried edible *Hypsizygus marmoreus* mushroom (100 g) were ground into powder and extracted with water at ˜10 ºC for 6 h (x 3, 1 L) under mechanical stirring. After filtration, the extracts were concentrated 12-fold, and precipitated with EtOH (3:1; v/v). The precipitate was collected by centrifugation (9000 rpm at 15 ºC for 10 min), and then dissolved in distilled water, dialyzed (Spectra/Por®; 12–14 kDa MWCO) with distilled water for 24 h to remove low-molecular-weight compounds, and freeze-dried (CW-*Hm*, 5.1 g).

The crude polysaccharide fraction (CW-*Hm*), previously dissolved in distilled water (˜ 10 mL), was subjected to freezing followed by mild thawing at 4 ºC, giving rise to a cold water-soluble (SCW-*Hm*, 3.7 g) and an insoluble fraction (ICW-*Hm*, 1.2 g), which were separated by centrifugation (9000 rpm, 15 ºC for 15 min).

SCW-*Hm* was further purified twice by treatment with Fehling solution (Jones & Stoodley, 1965) and the precipitated material (FP_2CW-*Hm*) was centrifuged off (9000 rpm at 20 ˚C for 15 min). FP_2CW-*Hm* was neutralized with HOAc, dialyzed with distilled water, deionized with strongly acidic cation exchange resin (Dowex ® 50WX2 hydrogen form), and freeze-dried (969 mg) (Fig. 1).

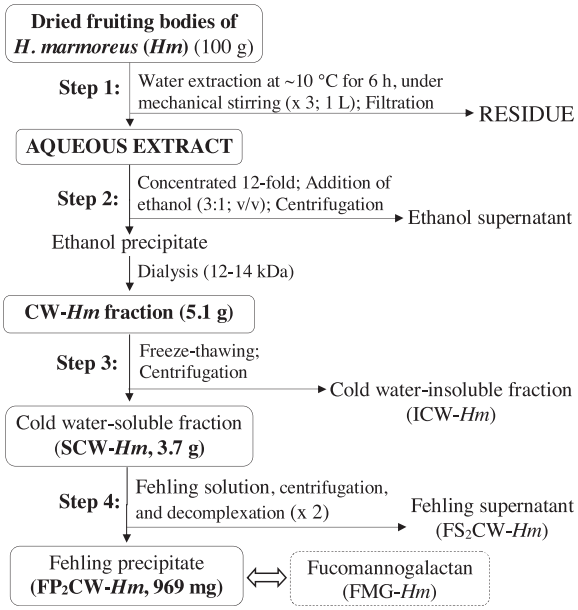

Fig. 1. Schematic diagram of extraction and purification of the heterogalactan from fruiting bodies of *Hypsizygus marmoreus* ("white" strain).

2.2. Determination of homogeneity and molecular weight of heteropolysaccharide

The homogeneity and average molecular weight (M_w) of FP_2CW-*Hm* were determined by high performance size exclusion chromatography (HPSEC) coupled to a Shimadzu RID-10A refractive index detector (RI) (Shimadzu Corporation, Kyoto, Japan). The chromatography system consisted of a Shimadzu LC-10AD HPLC pump, a manual injector valve (Shimadzu) fitted with a 200-µL loop and an Ultrahydrogel column (7.8 × 300 mm) system (Waters Corporation, Milford, United States) with exclusion limits of $7\times10^{6,}$ $^{4\times10^{5,}}$ $^{8}\times10^{4}$ and $5x10^{3}$ Da arranged in series. The mobile phase was 0.1 M $NaNO_3$ with sodium azide (0.03%), and a flow rate of 0.6 mL min^{-1}. The molecular weight was calculated by reference to a standard curve plotted according to the retention time and the logarithm of the respective molecular weight of the dextran standards. Data acquisition and analysis were carried out using LC solution software (Shimadzu Corporation, Kyoto, Japan).

A standard curve of dextran with molecular weights of 9.4, 22.8, 40.2, 60.0, 72.2, 150, 266, 410, and 670 kDa was built to determine the average molecular weight of the heteropolysaccharide.

2.3. Analysis of the monosaccharide composition

The monosaccharide composition was determined by gas chromatography-mass spectrometry (GC–MS) after derivatization to form alditol acetates (Wolfrom & Thompson, 1963a, 1963b). Briefly, the FP_2CW-*Hm* fraction (˜1 mg) was hydrolyzed with 2 M trifluoroacetic acid (TFA, 200 µL) at 100 ˚C for 8 h and converted to alditol acetates by successive $NaBH_4$ reduction (pH 9–10), and acetylation with Ac_2O-pyridine (1:1, v/v) for 12 h at room temperature. The GC–MS analysis was performed using an Agilent 7820A gas chromatograph coupled to an Agilent 5975E quadrupole mass spectrometer (Agilent Technologies, Santa Clara, United States) fitted with a split/splitless capillary inlet system, an Agilent G4513A autosampler, and a capillary HP5-MS column (30 m x 0.25 mm x 0.25 µm). Injections of 1 µL were made in the splitless mode at an injection temperature of 250 ˚C and the detector operating at 280 ºC, using helium as the carrier gas at a flow rate of 1 mL min^{-1}. The column oven temperature was initially held at 75 ˚C for 1 min, programmed at 35 ºC min^{-1} to 100 ºC (5 min), then 45 ºC min^{-1} to 150 ºC, hold for 5 min, 55 ºC min^{-1} to 200 ºC (15 min), and 65

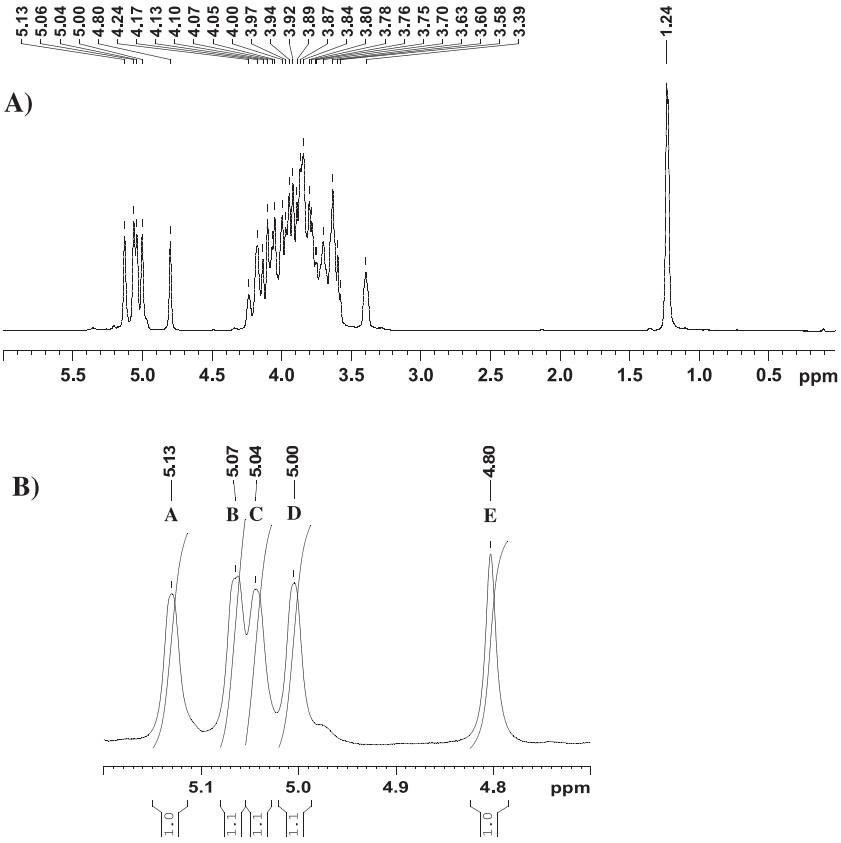

Fig. 2. ^{1}H NMR spectrum (500 MHz, D_2O, 50 °C) **(A)**, with an amplified insert of the anomeric region **(B)**, of the fucomannogalactan isolated from *H. marmoreus* (FMG-*Hm*).

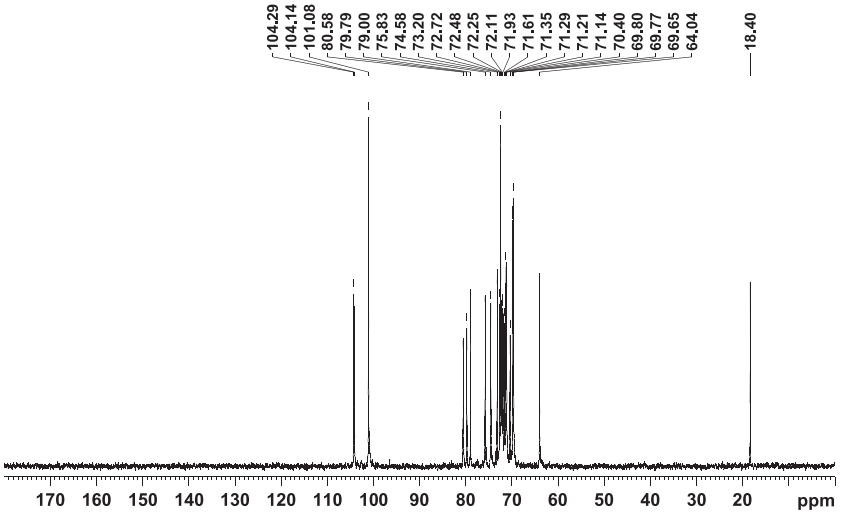

Fig. 3. ^{13}C NMR spectrum of fucomannogalactan from *H. marmoreus* (FMG-*Hm*), analyzed in D_2O at 70 °C.

ºC min^{-1} to 240 ºC (2 min). Electron impact (EI) analysis was performed with the ionization energy set at 70 eV. The compounds were identified by comparing the retention times and mass spectra of the samples with those of the standards.

2.4. Methylation analysis

Linkage analysis of sugars was performed by permethylation (Ciucanu & Kerek, 1984), conversion to the partially methylated alditol acetates (PMAAs) (Wolfrom & Thompson, 1963a, 1963b), and GC–MS analysis. Briefly, the sample (FP_2CW-*Hm*; ˜10 mg) was dissolved in dimethyl sulfoxide (Me_2SO; 500 µL), after which powdered NaOH (20 mg) and iodomethane (CH_3I; 500 µL) were added. After vigorous stirring for 30 min, the mixture was allowed to rest overnight at room temperature. The reaction was interrupted by the addition of water, neutralization with HOAc, and the products were isolated by partition between $CHCl_3$ and water. The organic layer containing the methylated product was washed in water several times and dried. The methylated polymer (1–2 mg) was hydrolyzed with 1 M TFA (200 µL) for 12 h at 100 ºC, followed by $NaBH_4$ reduction and acetylation as described above (item 2.3), yielding a mixture of partially *O*-methylated alditol acetates, which was analyzed by GC–MS. The injector temperature was

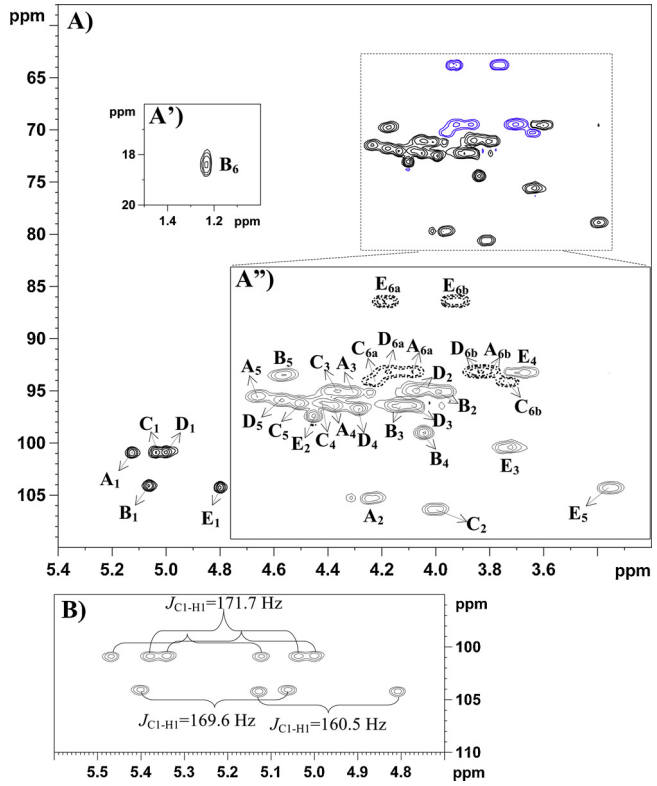

Fig. 4. HSQC-edit (A) and coupled HSQC spectra (B) of fucomannogalactan (FMG-*Hm*) from *H. marmoreus*, analyzed in D_2O at 50 °C. Amplified inserts of the C-6 region of Fuc*p* (A'), and carbinolic region (A") of the HSQC-edit experiment. **A** = 2,6-di-*O*-substituted α-Gal*p* residues; **B** = non-reducing end units of α-Fuc*p*; **C** = 2,6-di-*O*-substituted α-Gal*p* residues; **D** = 6-*O*-substituted α-Gal*p* residues; **E** = non-reducing end units of β-Man*p*.

Table 1
^{13}C and ^{1}H assignments of the fucomannogalactan from *H. marmoreus*.

Units	$^{1}H/^{13}C$ [a,b,c]						
	1	2	3	4	5	6a	6b
→ 2,6)-α-Gal*p*-(1→	101.06	***79.80***	71.25	72.34	71.55	***69.66***	
(Residue A)	5.13	***3.97***	4.01	4.06	4.24	***3.87***	***3.70***
α-Fuc*p*-(1→	104.14	71.20	72.36	74.58	69.81	18.36	
(Residue B)	5.07	*3.80*	3.89	3.85	4.18	1.24	
→ 2,6)-α-Gal*p*-(1→	101.01	***80.67***	71.13	72.07	72.10	***70.41***	
(Residue C)	5.04	***3.82***	4.05	4.08	4.14	***3.96***	***3.64***
→ 6)-α-Gal*p*-(1→	101.00	71.03	72.30	72.55	71.85	***69.79***	
(Residue D)	5.00	3.82	3.87	4.00	4.20	***3.93***	***3.72***
β-Man*p*-(1→	104.29	73.16	75.65	69.64	78.96	63.86	
(Residue E)	4.80	4.11	3.64	3.61	3.40	3.94	3.76

[a] Assignments were based on ^{1}H, ^{13}C, HSQC-edit, HSQC-TOCSY, HSQC-NOESY, and 2D-NOESY spectra.
[b] The values of chemical shifts were recorded with reference to TSP-d_4 as internal standard.
[c] The values highlighted in bold correspond to *O*-substitutions.

kept at 250 ºC, with the oven temperature increasing from 75 ºC (held for 1 min) to 100 ºC (35 ºC min^{-1}, then held for 5 min), 150 ºC (45 ºC min^{-1}, then held for 5 min), 200 ºC (55 ºC min^{-1}, then held for 15 min), 250 ºC (65 ºC min^{-1}, then held for 10 min), and to 270 ºC (50 ºC min^{-1} and held for 10 min). Partially *O*-methylated alditol acetates were identified from the *m/z* of their positive ions, by comparison with standards (Sassaki, Gorin, Souza, Czelusniak, & Iacomini, 2005). The relative percentage of the resulting PMAAs was estimated as the ratio of the peak areas using the Agilent ChemStation software (Agilent Technologies, Santa Clara, United States).

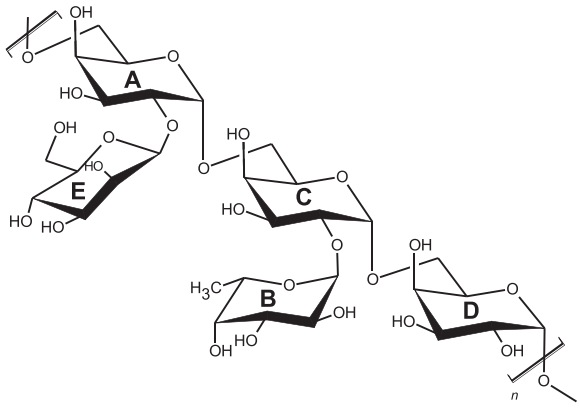

Fig. 5. Proposed structure of the heteropolysaccharide FMG-*Hm* from *H. marmoreus*.

2.5. Nuclear magnetic resonance (NMR) spectroscopy

All the NMR measurements were acquired in a 11.75 T (500 MHz for hydrogen frequency) (Bruker Corporation, Billerica, Massachusetts, United States) using a temperature of 323 K, TSP-d_4 as an internal reference, solvent D_2O and the inverse detection probe head, with the exception of the ^{13}C experiment that was performed at 343 K on a broadband probe.

The ^{1}H NMR spectra with HDO presaturation signal, using continuous wave, were performed using the following parameters: spectral width, 10,000 Hz; 9.8 μs for 90° pulse; acquisition time, 3.27 s; relaxation delay, 0.1 s; and 64 scans. ^{13}C NMR spectrum was acquired using: spectral width, 31,250 Hz; 9.5 μs for 90° pulse time, acquisition time of 0.52 s; relaxation delay, 0.1 s, and 4K scans.

For heteronuclear correlation experiments (HSQC-edit, HSQC-TOCSY, HSQC-NOESY) were used: F_1 spectral width, 10,000 Hz; F_2 spectral width, 31,250 Hz; relaxation delay, 1.5 s; number of experiments in F_1, 256; acquisition time in F2, 0.27s; and mixing time of 10 ms (HSQC-TOCSY) or 25 ms (HSQC-NOESY).

All the data were processed using *TopSpin* software (Bruker Corporation, Billerica, Massachusetts, United States).

2.6. Cell culture

The B16-F10 murine melanoma cell line was obtained from the Rio de Janeiro Cell Bank (Brazil). B16-F10 cells were stored at 37 °C in a humidified atmosphere containing 5% CO_2in DMEM – Dulbecco's Modified Eagle's Medium Powder, high glucose, pyruvate, supplemented with 10% fetal bovine serum, sodium bicarbonate (1.5 g L^{-1}) and 0.25 μg mL^{-1} penicillin-streptomycin in 0.85% saline. The experiments were performed with cells in passages from 1 to 5 and 70 to 90% cell confluence.

2.7. Neutral red and violet crystal assays

The neutral red uptake assay was performed as previously described (ICCVAM, 2006; ISO, 2009; Repetto, Del Peso, & Zurita, 2008). Briefly, B16-F10 cells were seeded in a 96-well tissue culture plate at a density of 600 per well, and the microplate was then incubated for 24 h at 37 °C in a 5% CO_2 incubator. Thereafter, the cells were exposed to different concentrations of the polysaccharide FMG-*Hm* (1, 10, and 100 μg mL^{-1}) for 72 h in a 5% CO_2 incubator at 37 °C. At the end of the incubation period, the neutral red solution was added to each well at a final concentration of 100 μg mL^{-1}. After 2 h of incubation, the supernatant was discarded and replaced with acidified ethanol solution (100 μL; 1% acetic acid in 50% ethanol) to extract the dye from the cells, which was measured at 550 nm in a spectrophotometric plate reader (BioTek® Instruments, Inc., Winooski, United States).

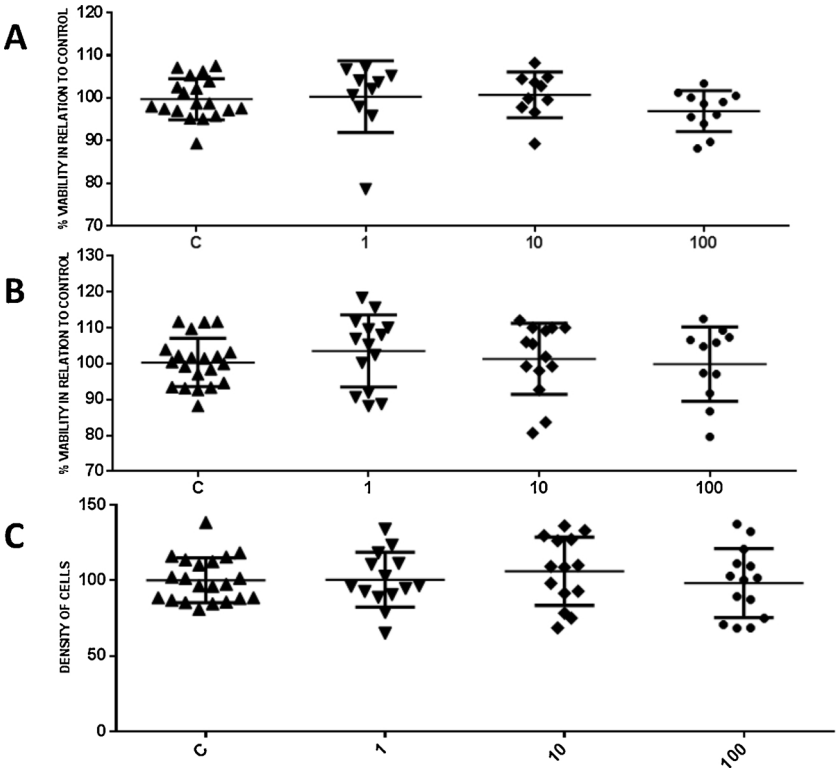

Fig. 6. FMG-*Hm* is non-cytotoxic to B16-F10 cells. Melanoma cells were treated with fucomannogalactan (1, 10, and 100 μg mL^{-1}) for 72 h. The cell viability was tested by neutral red **(A)**; MTT **(B)**; and cell density by crystal violet **(C)**. Data are represented as mean ± SD of three independent experiments performed in quadruplicate, statistical analysis: One-way ANOVA, $p > 0.05$ compared with the control group.

Cell density was evaluated by staining residual cells adhered on the microplate were stained with 0.25 mg mL^{-1} crystal violet solution for 20 min. Next, the microplate was washed twice with water, and the dye was eluted with 33% aqueous acetic acid solution. The absorbance of each well was determined spectrophotometrically at 540 nm using a microplate reader (Bonnekoh, Wevers, Jugert, Merk, & Mahrle, 1989; Vega-Avila & Pugsley, 2011).

2.8. MTT assay

The MTT assay was based on the method described by Mosmann (1983). B16-F10 cells were plated in a 96-well culture plate (600 cells/well) and incubated for 24 h. The cells were then treated with the polysaccharide sample at 1, 10, and 100 μg mL^{-1} for 72 h. To observe cell viability by mitochondrial enzymes, MTT solution was added over a 3-hour period to reach a final concentration of 50 μg mL^{-1}. At the end of the incubation period, the medium with MTT was discarded and the purple formazan crystals formed were diluted with dimethyl sulfoxide (100 μL per well). The absorbance values were measured at 550 nm in a microplate spectrophotometer.

2.9. Colony forming cell assay

A colony forming cell assay or clonogenic assay was performed, using the method proposed by Franken, Rodermond, Stap, Haveman, and van Bree (2006). After pre-incubation for 24 h, B16-F10 cells (12×10^3 cells/well) were treated with FMG-*Hm* (100 μg mL^{-1}) at 37 ºC for 72 h. Cells were re-plated onto a 6-well cell culture plate (500 cells/well) and incubated for 96 h, with the culture medium replaced after 72 h. At the end of the colony-forming period, the cells were fixed in acidic ethanol solution (2% acetic acid in 50% ethanol), washed with ultrapure water and stained using crystal violet. The cell colonies on the plates were photographed and counted using *ImageJ* software (Schneider, Rasband, & Eliceiri, 2012).

2.10. Cell morphological analysis by confocal microscopy

The B16-F10 melanoma cells were cultured on glass coverslips and then incubated with 100 μg mL^{-1} polysaccharide for 72 h. Thereafter, exposed and non exposed cells (control) were fixed in 2% paraformaldehyde for 30 min, washed with phosphate buffered saline (PBS), and loaded with ActinGreen™ ReadyProbes® reagent (1:40) and DAPI (1:1000 in 0.01% saponin-PBS) for 40 min. Coverslips were washed and mounted in Fluoromount™ medium. Stained cells were examined using confocal microscopy (Nikon A1R-MP laser scanning confocal microscope) (Nikon Corporation, Tokyo, Japan).

2.11. Measurement of cell migration

B16-F10 cells were seeded at a density of 500 cells per well in a 6-well plate, and kept overnight in a CO_2 incubator overnight. The cells were then treated with 100 μg L^{-1} of FMG-*Hm* for 72 h. An additional cell culture without FMG-*Hm* was used as control. After reaching the required confluence, monolayers were scratched mechanically with a sterile pipette tip. The "wound closure" phenomenon was monitored by means of confocal microscopy (Nikon A1R-MP laser scanning confocal microscope) (Nikon Corporation, Tokyo, Japan) under 100x magnification, and images of the same areas were recorded at 30 min intervals for 23.5 h (Liang, Park, & Guan, 2007). The percentage of the scratch open area was measured using *TScratch* software (Gebäck, Schulz, Koumoutsakos, & Detmar, 2009).

3. Results and discussion

3.1. Structural characterization of the fucomannogalactan (FMG-Hm)

The polysaccharide FP_2CW-*Hm* was purified according to the procedure outlined in Fig. 1. HPSEC-RID analysis (Fig. 1S) indicated that FP_2CW-*Hm* had a single symmetrical peak (M_w/M_n 1.08), with a M_w 17.1 kDa, containing fucose, mannose, and galactose as monosaccharide components in an area ratio of 1:1.08:3.17 (Fig. 2S),

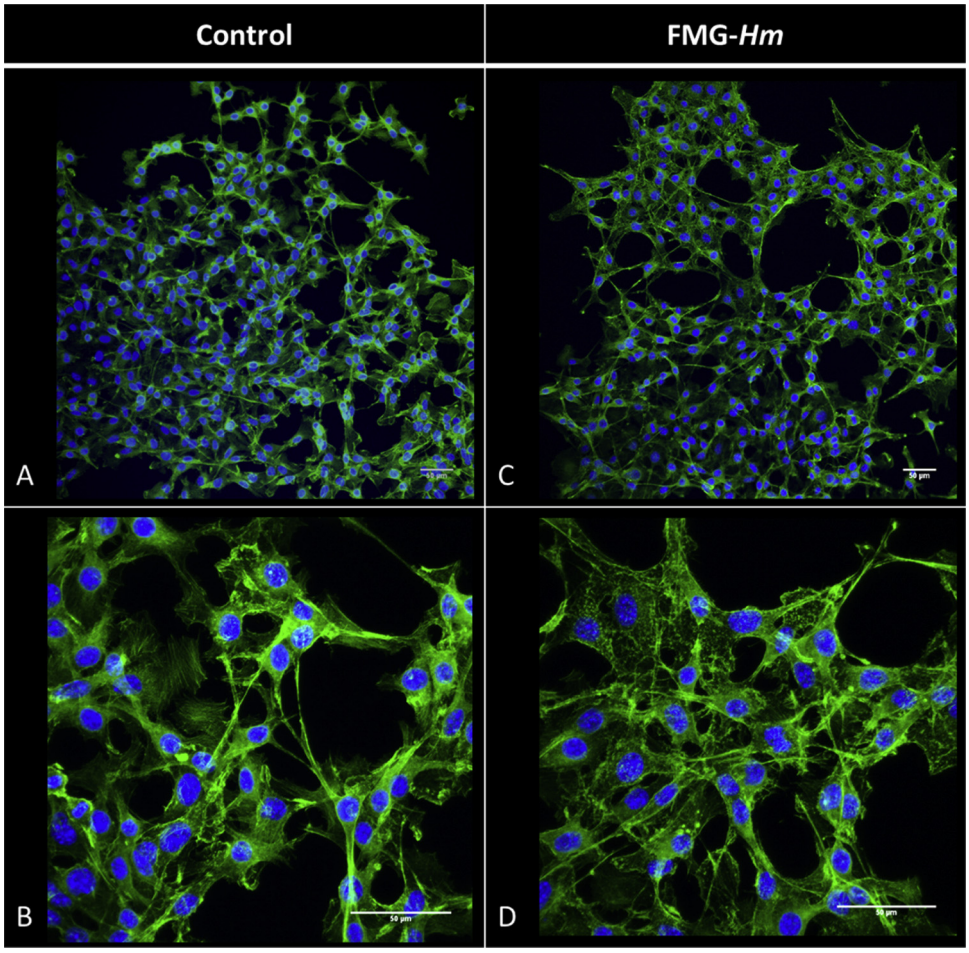

Fig. 7. FMG-*Hm* does not change cell morphology. B16-F10 cells were exposed to FMG-*Hm* (100 μg mL^{-1}) for 72 h. These assays were performed as three independent experiments. Confocal microscopy: A, B (control); C e D (treated). Scale bar: 50 μm; blue staining: DAPI highlights the nucleus; green staining: ActinGreen™ ReadyProbes® reagent to visualize the actin cytoskeleton.

suggesting the presence of a fucomannogalactan, which was named FMG-*Hm*.

Methylation analysis was performed to identify the types of glycosyl linkages present in FMG-*Hm* (Fig. 3S). A GC—MS analysis of the resulting partially methylated alditol acetates revealed four peaks in an area ratio of 1:1.04:1.14:2.14, corresponding to 2,3,4-tri-*O*-methyl-fucose, 2,3,4,6-tetra-*O*-methyl-mannose, 2,3,4-tri-*O*-methyl-galactose, and 3,4-di-*O*-methyl-galactose, respectively. These data suggested that FMG-*Hm* consists of a branched structure, containing non-reducing end groups of Man*p* and Fuc*p*, and 6-*O*- and 2,6-di-*O*-substituted Gal*p* units.

The anomeric region of the ^{1}H NMR spectrum of FMG-*Hm* (Fig. 2) presented 5 distinctive signals at δ 5.13, 5.07, 5.04, 5.00, and δ 4.80, which were dubbed A to E, respectively. In the ^{13}C NMR spectrum (Fig. 3), only three anomeric carbon signals were visible at δ 104.29, 104.14, and δ 101.11, attributed to overlapping, which were resolved in the HSQC-DEPT experiment (Fig. 4A). The anomeric region showed C1/H1 signals at δ 101.06/5.13 (A), 104.14/5.07 (B), 101.01/5.04 (C), 101.00/5.00 (D), and 104.29/4.80 (E), indicating a α-configuration for residues A to D, and β- for residue E. The glycosidic configurations were confirmed by values of the coupling constants $J_{C\text{-}1,H\text{-}1}$ found in $^{1}H/^{13}C$ coupled HSQC spectra (Fig. 4B). The non-reducing ends of Man*p* (Residue E) had a β-configuration due to the value of 160.5 Hz, while those of Gal*p* (Residues A, C, and D) and Fuc*p* (Residue B) had α-configuration, consistent with the $J_{C\text{-}1,H\text{-}1}$ = 171.7 and 169.6 Hz, respectively (Agrawal, 1992). The

The absolute configurations of the monosaccharides were attributed by comparison with previous data obtained for a similar polymer (Carbonero et al., 2008; Komura et al., 2010), which showed that galactose and mannose residues had the D- and the fucose residue the L-configuration.

Additional NMR experiments, HSQC-TOCSY (Fig. 4S), HSQC-NOESY (Fig. 5 S A), and 2D-NOESY (Fig. 5S B), were performed to elucidate the structure of this heterogalactan (FMG-Hm). The connectivities observed in the HSQC-TOCSY (Fig. 4S) experiment allowed us to assign all the carbons and protons of each unit. Once the protons were identified, chemical shifts of their corresponding carbons were confirmed by HSQC-edit analysis (Fig. 4A; Table 1). Based on NMR analyses, the identities of monosaccharide residues were established (Table 1), which are in agreement with the literature data of similar heterogalactans isolated from other basidiomycetes (Carbonero et al., 2008; Ruthes et al., 2013)

The downfield shifts of the C-2 (A: δ 79.80; and C: δ 80.67) and C-6 (A: 69.66; and C: 70.41) signals indicated that residues A and C were 2,6-linked α-D-galactopyranosyl units. Residue B was identified as an α-linked terminal L-fucopyranosyl unit. This was strongly supported by the appearance of a proton signal at δ 1.25 and a carbon signal at δ 18.36 for a CH_3 group. The carbon chemical shifts of residue B from C-1 to C-6 corresponded almost exactly to the standard values of methyl glycosides (Agrawal, 1992). In residue D, the downfield shift of the C-6 signal (δ 69.79), inverted in the HSQC-DEPT spectrum, confirmed the presence of 1,6-linked α-D-galactopyranosyl unit. Residue E was identified as a β-linked terminal D-mannopyranosyl unit due to the C-1 to C-6 values closely to the standard values of methyl glycosides (Agrawal, 1992).

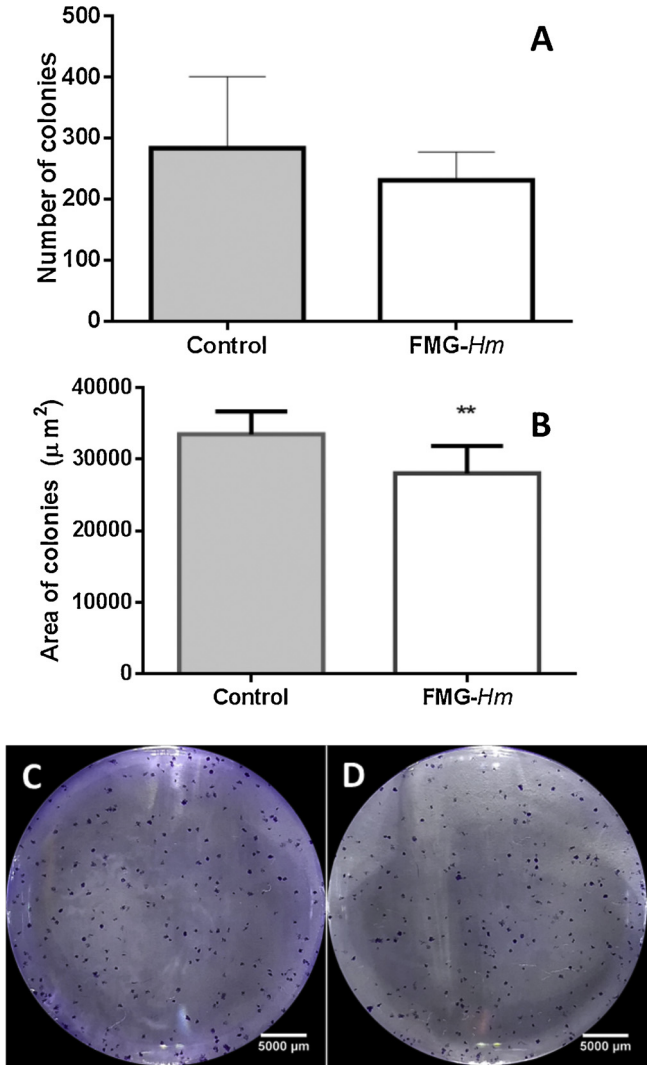

Fig. 8. Effects of FMG-*Hm* on colony formation of B16-F10 cells. B16-F10 cells were treated with FMG-*Hm* (100 μg mL^{-1}) for 72 h and then re-plated. After incubation for 96 h, colonies were fixed, stained and visualized. Quantitative data on the number (A) and size (B) of each colony formed, as well as the control images (C) and cells treated with polysaccharide (D), are shown above. Data are presented as mean ± SD of two repetition, from five independent studies. Data were analyzed with a *t*-test and the Mann-Whitney post-test (** $p = 0.0022$).

The sequence of the residues in the repeating unit was established based on HSQC-NOESY and 2D-NOESY experiments (Fig. 5S, Table 1S). In the HSQC-NOESY spectrum, the inter-residue contacts **E** H-1/**A** C-2, and **B** H-1/**C** C-2 confirmed the O-2 substitution of α-Gal*p* units (Residues **A** and **C**) by a single units of β-Man*p* (Residue **E**) and α-Fuc*p* (Residue **B**), respectively. The inter-residual connectivities **A** H-1/**C** H-6a, **C** H-1/**D** H-6a, and **D** H-1/**A** H-6b in the 2D-NOESY spectrum recognized the following sequence of 6-*O*-substituted α-Gal*p* units from the main chain (Residues **A**, **C**, and **D**): **A**(1→6)**C**, **C**(1→6)**D**, and **D**(1→6)**A**.

Thus, from the above chemical and NMR experiment results, it was found to be the one reported in Fig. 5:

Heterogalactans containing fucose and mannose side chains have commonly been described in mushrooms. However, most of them were substituted mainly for disaccharide 3-*O*-α-D-Man*p*-α-L-Fuc*p* and non-reducing end groups of α-L-Fuc*p*.

Fucomannogalactans similar to those found in the FMG-*Hm* fraction have previously been isolated from *Lentinus edodes* (Carbonero et al., 2008) and *Amanita muscaria* (Ruthes et al., 2013), which showed anti-inflammatory and/or antinociceptive effects.

3.2. Biological effects of the fucomannogalactan (FMG-Hm)

3.2.1. Fucomannogalactan isolated from H. marmoreus (FMG-Hm) is non-cytotoxic to B16-F10 cells

In this work, to investigate the cytotoxicity of the heteropolysaccharide treatment on B16-F10 cells, melanoma cells were incubated with FMG-*Hm* at various concentrations (1, 10, and 100 μg mL^{-1}) for 72 h and cell viability was determined by the neutral red and MTT assays. As shown in Fig. 6A and B, after treatment with polysaccharide, cell viability was not significantly changed compared to that of untreated control cells.

FMG-*Hm* was then tested to determine its ability to cause differences in B16-F10 cells density, using the crystal violet technique. As can be seen in Fig. 6C, FMG-*Hm* did not affect melanoma cell density, since the treated and control groups are the same.

With this set of experiments, we were able to demonstrate that FMG-*Hm* is non-toxic and does not alter the cell density under these conditions. However, it should be noted that there have been studies using natural products with direct pharmacological *in vitro* and *in vivo* effects on melanoma (AlQathama & Prieto, 2015). In addition, the polysaccharides obtained from edible mushrooms show antitumor activity against several types of cancer, such as the kidney (Yang et al., 2013), breast (Novaes, Valadares, Reis, Gonçalves, & Menezes, 2011), and melanoma (Hung, Hsu, Chang, & Chen, 2012).

3.2.2. B16-F10 morphology is maintained after treatment with fucomannogalactan (FMG-Hm)

Morphology is an important marker for assessing the state of cell culture, indicating viable or suffering cells. After treatment, the morphology of B16-F10 cells was evaluated by labeling of actin (green fluorescence from ActinGreen™ ReadyProbes®) and nuclei (blue fluorescence). No change in morphology (spindle-shaped and epithelial-like cells) was observed between the control group and the group treated with 100 μg mL^{-1} after 72 h of treatment. The cells remained stacked one above the other, with the same spreading pattern and confluence, forming a cell monolayer, as shown below in Fig. 7.

Thus, as seen here the absence of changes in morphology may be another indication that the tested polysaccharide has a non-toxic effect. Then the next step was to assess colony formation from testing our hypothesis.

3.2.3. Colony formation decreases after treatment with fucomannogalactan (FMG-Hm)

The clonogenic assay allows for the evaluation of the colony forming ability of a single cell, without the stimulus of contact with neighboring cells, since unlimited proliferation is the predominant feature of all tumoral cells. The support of proliferative signaling and the suppression by growth suppressors are defined by the number of viable cells or the maintenance of proliferative capacity over time (Menyhárt et al., 2016), in the presence or absence of treatment.

The colony forming ability and the area of each colony were evaluated using B16-F10 cells, treated or not (control) with FMG-*Hm* at 100 μg mL^{-1} for 72 h. An analysis of this assay indicated that the number of colonies remained the same in both groups (treated and control), but surprisingly, the mean colony size in the FMG-*Hm* treated group was decreased (** $p = 0.0022$), as demonstrated in Fig. 8.

The inhibition in colony formation caused by exposure to FMG-*Hm* may be associated with other promising effects, as discussed in the literature. A polysaccharide obtained from the fungus *Rhizopus nigricans* was able to decrease the formation of colonies of the BGC-823 cell line of stomach cancer in concentrations of 200, 400, and 600 μg mL^{-1}. The same polymer induced G2/M phase cell cycle arrest and apoptotic cell death through the mitochondrial pathway in BGC-823 cells (Chen et al.,

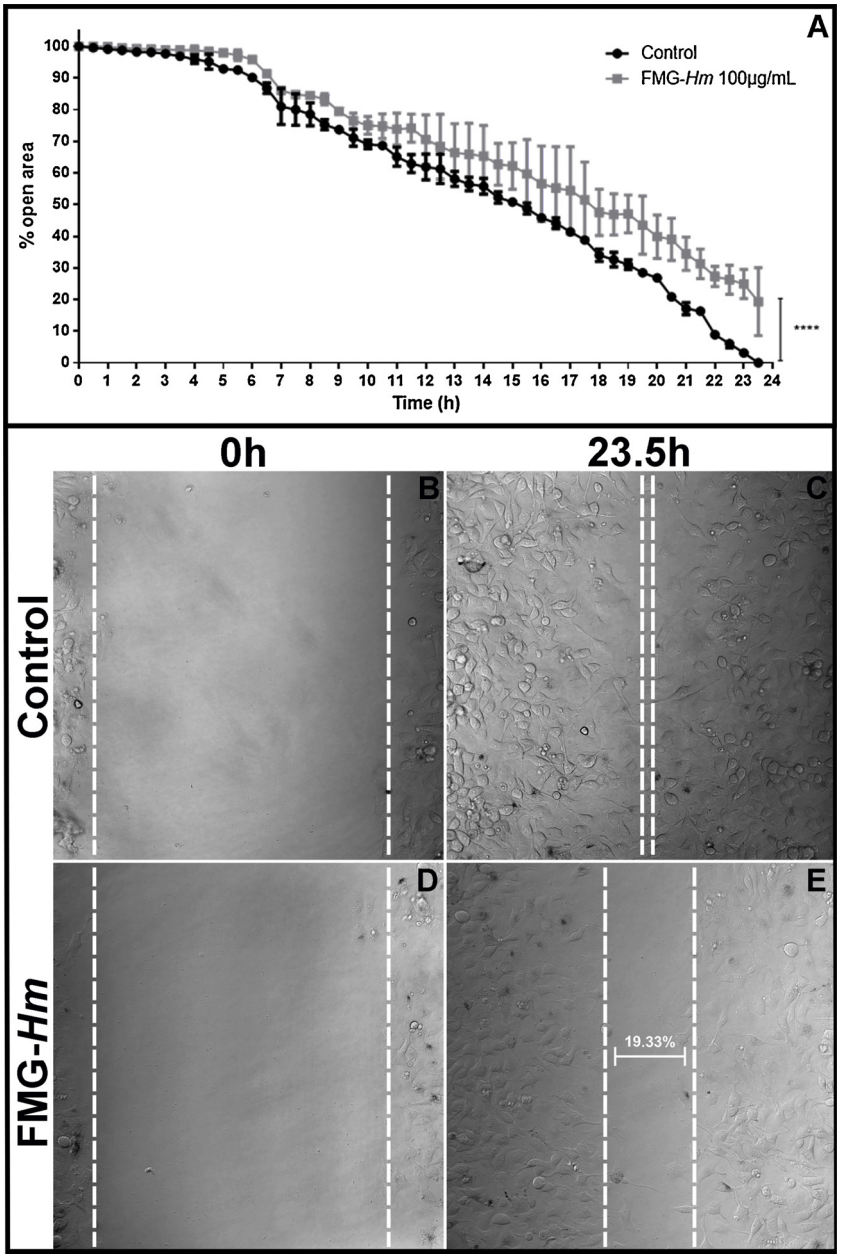

Fig. 9. FMG-*Hm* interferes with the migration ability of B16-F10 cells. B16F10 cell monolayers were incubated with 100 µg mL^{-1} of FMG-*Hm* or not (control) for 72 h and then carefully scratched using sterilized pipette tips. After removing detached cells, the "wound closure" phenomenon was monitored at 30 min intervals for 23.5 h by confocal microscopy. The data represent the mean ± SD of three independent experiments. Statistical analysis: Unpaired *t*-test (****$p < 0.0001$).

2013).

This result is interesting because it shows the difference in cell growth, such as: a) cells grow in groups (Fig. 6C), exchanging signals and growth stimuli, adhesion cell-cell and cell-MEC; or b) grow isolated, without external stimuli, only with their ability to survive (Fig. 8B). We see here that although the treatment does not alter the proliferation, it compromises the ability of the cells to form colonies when they grow individually. Therefore, the next step was to evaluate alterations in the malignancy capacity.

3.2.4. Fucomannogalactan (FMG-Hm) reduces cell migration

The next biological event to be evaluated was cell migration, since one of the defining characteristics of cancer is the rapid growth of abnormal cells that extend beyond their usual limits of origin and then invade other parts of the body in a process known as metastasis, which is the main cause of death in patients (WHO, 2016). For metastasis to occur, several cellular and extracellular events are necessary to enable the cancer cells to migrate (Zhou, Yang, Andl, Wickett, & Zhang, 2015).

Cell migration is a key event in tumor progression, defining the ability of cells to perform metastasis. In Fig. 9, note that the group of cells treated with FMG-Hm reduced the cell migration ability remarkably ($p < 0.0001$) in comparison to the control group (untreated). After 23.5 h, the control group was already completely closed (confluent), while the treated group still had an average of 19.33% of the open area, indicating that FMG-Hm reduced cell migration.

These amazing results of migration reduction and colony formation are promising for a new antitumoral therapy. The results are consistent with FMG-*Hm*effects on morphology (Fig. 7). In addition, an immune-staining technique that stains actin filaments (green) and nuclei (blue) was performed to visualize the B16-F10 cell morphology, which revealed no change in cell morphology between treated (100 µg mL^{-1} FMG-*Hm* for 72 h) and control groups.

Melanoma cells remained stacked upon each other, with the same spread pattern and confluence in the formation of the cell layer as shown in Fig. 7. The results of this study corroborate these findings, since they indicate that the fucomannogalactan evaluated here caused no toxic effects nor did it alter the cellular morphology. However, it did alter melanoma cells, reducing the colony forming ability and reducing cellular migration, without altering cell proliferation.

Thus, our hypothesis was confirmed, and the new isolated molecule of the mushroom *Hypsizygus marmoreus*, presented antimelanoma activity, without causing toxicity.

In conclusion, these data demonstrate that this newly characterized polysaccharide is a promising tool for antimelanoma therapy, although further studies are needed to shed light on its antitumor effect.

Acknowledgements

The authors would like to thank the YUKI Cogumelos Company (Owner: José Francisco Ramos Fernandes Viana) for supplying the biological material. This study was partly financed by the Coordenação de Aperfeiçoamento de Pessoal de Nível Superior - Brasil (CAPES) - Finance Code 001", and Conselho Nacional de Desenvolvimento Científico e Tecnológico (CNPq).

Appendix A. Supplementary data

Supplementary material related to this article can be found, in the online version, at doi:https://doi.org/10.1016/j.carbpol.2019.115203.

References

Agrawal, P. K. (1992). NMR Spectroscopy in the structural elucidation of oligosaccharides and glycosides. *Phytochemistry, 31*(10), 3307–3330.
AlQathama, A., & Prieto, J. M. (2015). Natural products with therapeutic potential in melanoma metastasis. *Natural Product Reports, 32*(8), 1170–1182.
Biscaia, S. M. P., Carbonero, E. R., Bellan, D. L., Borges, B. S., Costa, C. R., Rossi, G. R., et al. (2017). Safe therapeutics of murine melanoma model using a novel anti-neoplasic, the partially methylated mannogalactan from *Pleurotus eryngii*. *Carbohydrate Polymers, 178*, 95–104.
Bonnekoh, B., Wevers, A., Jugert, F., Merk, H., & Mahrle, G. (1989). Colorimetric growth assay for epidermal cell cultures by their crystal violet binding capacity. *Archives of Dermatological Research, 281*(7), 487–490.
Carbonero, E. R., Gracher, A. H. P., Komura, D. L., Marcon, R., Freitas, C. S., Baggio, C. H., et al. (2008). *Lentinus edodes* heterogalactan: Antinociceptive and anti-inflammatory effects. *Food Chemistry, 111*, 531–537.
Chen, G., Zhang, P., Huang, T., Yu, W., Lin, J., Li, P., et al. (2013). Polysaccharides from *Rhizopus nigricans* mycelia induced apoptosis and G2/M arrest in BGC-823 cells. *Carbohydrate Polymers, 97*(2), 800–808.
Ciucanu, I., & Kerek, F. (1984). A simple and rapid method for the permethylation of carbohydrates. *Carbohydrate Research, 131*, 209–217.
Franken, N. A. P., Rodermond, H. M., Stap, J., Haveman, J., & van Bree, C. (2006). Clonogenic assay of cells in vitro. *Nature Protocols, 1*(5), 2315–2319.
Gebäck, T., Schulz, M. M., Koumoutsakos, P., & Detmar, M. (2009). TScratch: A novel and simple software tool for automated analysis of monolayer wound healing assays. *Biotechniques, 46*(4), 265–274.
Hamidi, H., Pietilä, M., & Ivaska, J. (2016). The complexity of integrins in cancer and new scopes for therapeutic targeting. *British Journal of Cancer, 115*(9), 1017–1023.
Hanahan, D., & Weinberg, R. A. (2000). The hallmarks of cancer. *Cell, 100*(1), 57–70.
Hanahan, D., & Weinberg, R. A. (2011). Hallmarks of cancer: The next generation. *Cell, 144*(5), 646–674.
Hung, C., Hsu, B., Chang, S., & Chen, B. (2012). Antiproliferation of melanoma cells by polysaccharide isolated from *Zizyphus jujuba*. *Nutrition, 28*(1), 98–105.
ICCVAM - Interagency Coordinating Committee on the Validation of Alternative Methods (2006). *Test method evaluation report: In vitro cytotoxicity test methods for estimating starting doses for acute oral systemic toxicity tests. (NIH Publication n°. 07-4519)*.
ISO - International Organization for Standardization (2009). *Biological evaluation of medical devices. Part 5: Tests for in vitro citotoxicity (ISO10993-5)*.
Ivanova, T. S., Krupodorova, T. A., Barshteyn, V. Y., Artamonova, A. B., & Shlyakhovenko, V. A. (2014). Anticancer substances of mushroom origin. *Experimental Oncology, 36*(2), 58–66.
Jones, J. K. N., & Stoodley, R. J. (1965). Fractionation using copper complexes. *Methods in Carbohydrate Chemistry, 5*, 36–38.
Komura, D. L., Carbonero, E. R., Gracher, A. H. P., Baggio, C. H., Freitas, C. S., Marcon, R., et al. (2010). Structure of *Agaricus* spp. fucogalactans and their anti-inflammatory and antinociceptive properties. *Bioresource Technology, 101*, 6192–6199.
Liang, C., Park, A. Y., & Guan, J. (2007). In vitro scratch assay: A convenient and inexpensive method for analysis of cell migration in vitro. *Nature Protocols, 2*(2), 329–333.
Lu, P., Weaver, V. M., & Werb, Z. (2012). The extracellular matrix: A dynamic niche in cancer progression. *Journal of Cell Biology, 196*(4), 395–406.
Ma, G., Yang, W., Mariga, A. M., Fang, Y., Ma, N., Pei, F., et al. (2014). Purification, characterization and antitumor activity of polysaccharides from *Pleurotus eryngii* residue. *Carbohydrate Polymers, 114*, 297–305.
Maverakis, E., Cornelius, L. A., Bowen, G. M., Phan, T., Patel, F. B., Fitzmaurice, S., et al. (2015). Metastatic melanoma - a review of current and future treatment options. *Acta Dermato Venereologica, 95*(5), 516–524.
Meng, X., Liang, H., & Luo, L. (2016). Antitumor polysaccharides from mushrooms: A review on the structural characteristics, antitumor mechanisms and immunomodulating activities. *Carbohydrate Research, 424*, 30–41.
Menyhárt, O., Harami-Papp, H., Sukumar, S., Schäfer, R., Magnani, L., De Barrios, O., et al. (2016). Guidelines for the selection of functional assays to evaluate the hallmarks of cancer. *Biochimica et Biophysica Acta Journal, 1866*, 300–319.
Milhorini, S. S., Smiderle, F. R., Biscaia, S. M. P., Rosado, F. R., Trindade, E. S., & Iacomini, M. (2018). Fucogalactan from the giant mushroom *Macrocybe titans* inhibits melanoma cells migration. *Carbohydrate Polymers, 190*, 50–56.
Mosmann, T. (1983). Rapid colorimetric assay for cellular growth and survival: Application to proliferation and cytotoxicity assays. *Journal of Immunological Methods, 65*, 55–63.
Novaes, M. R. C. G., Valadares, F., Reis, M. C., Gonçalves, D. R., & Menezes, M. C. (2011). The effects of dietary supplementation with Agaricales mushrooms and other medicinal fungi on breast cancer: Evidence-based medicine. *Clinics, 66*(12), 2133–2139.
Oliveira, G. K. F. O., Silva, E. V. S., Ruthes, A. C., Lião, L. M. L., Iacomini, M., & Carbonero, E. R. (2018). Chemical structure of a partially 3-*O*-methylated manno-fucogalactan from edible mushroom *Grifola frondosa*. *Carbohydrate Polymers, 187*, 110–117.
Ren, L., Perera, C., & Hemar, Y. (2012). Antitumor activity of mushroom polysaccharides: A review. *Food & Function, 3*, 1118–1130.
Ren, D., Wang, N., Guo, J., Yuan, L., & Yang, X. (2016). Chemical characterization of *Pleurotus eryngii* polysaccharide and its tumor-inhibitory effects against human hepatoblastoma HepG-2 cells. *Carbohydrate Polymers, 138*, 123–133.
Repetto, G., Del Peso, A., & Zurita, J. L. (2008). Neutral red uptake assay for the estimation of cell viability/cytotoxicity. *Nature Protocols, 3*(7), 1125–1131.
Ruthes, A. C., Carbonero, E. R., Córdova, M. M., Baggio, C. H., Sassaki, G. L., Gorin, P. A. J., et al. (2013). Fucomannogalactan and glucan from mushroom *Amanita muscaria*: Structure and inflammatory pain inhibition. *Carbohydrate Polymers, 98*, 761–769.
Sassaki, G. L., Gorin, P. A. J., Souza, L. M., Czelusniak, P. A., & Iacomini, M. (2005). Rapid synthesis of partially *O*-methylated alditol acetate standards for GC-MS: Some relative activities of hydroxyl groups of methyl glycopyranosides on Purdie methylation. *Carbohydrate Research, 340*, 731–739.
Schneider, C. A., Rasband, W. S., & Eliceiri, K. W. (2012). NIH Image to ImageJ: 25 years of image analysis. *Nature Methods, 9*, 671–675.
Srinivasahan, V., & Durairaj, B. (2015). In vitro and apoptotic activity of polysaccharide rich *Morinda citrofolia* fruit on MCF-7 cells. *Asian Journal of Pharmaceutical and Clinical Research, 8*(2), 190–193.
Theocharis, A. D., Skandalis, S. S., Gialeli, C., & Karamanos, N. K. (2016). Extracellular matrix structure. *Advanced Drug Delivery Reviews, 97*, 4–27.
Tong, H., Xia, F., Feng, K., Sun, G., Gao, X., Sun, L., et al. (2009). Structural characterization and in vitro antitumor activity of a novel polysaccharide (POPS-1) isolated from the fruiting bodies of *Pleurotus ostreatus*. *Bioresource Technology, 100*(4), 1682–1686.
Vega-Avila, E., & Pugsley, M. K. (2011). An overview of colorimetric assay methods used to assess survival or proliferation of mammalian cells. *Proceedings of the Western Pharmacology Society, 54*, 10–14.
WHO. World Health Organization - Cancer (2016). Retrieved August 22, 2016, from http://www.who.int/mediacentre/factsheets/fs297/en/.
Wolfrom, M. L., & Thompson, A. (1963a). Reduction with sodium borohydride. *Methods in Carbohydrate Chemistry, 2*, 65–68.
Wolfrom, M. L., & Thompson, A. (1963b). Acetylation. *Methods in Carbohydrate Chemistry, 2*, 211–215.
WCRF International- World Cancer Research Fund International - Skin cancer statistics. (2019). Retrieved January 22, 2019, from https://www.wcrf.org/dietandcancer/cancer-trends/skin-cancer-statistics.
Yang, Z., Xu, J., Fu, Q., Fu, X., Shu, T., Bi, Y., et al. (2013). Antitumor activity of a polysaccharide from *Pleurotus eryngii* on mice bearing renal cancer. *Carbohydrate Polymers, 95*(2), 615–620.
Zhou, L., Yang, K., Andl, T., Wickett, R. R., & Zhang, Y. (2015). Perspective of targeting cancer-associated fibroblasts in melanoma. *Journal of Cancer, 6*(8), 717–726.
Zong, A., Cao, H., & Wang, F. (2012). Anticancer polysaccharides from natural resources: A review of recent research. *Carbohydrate Polymers, 90*(4), 1395–1410.